QUASI-STATIC DESIGN OF SHARED MOORING SYSTEMS FOR FLOATING OFFSHORE WIND FARMS

Marcus Vinicius Biroli
Centre for Marine Technology and Engineering (CENTEC), Instituto Superior Técnico, University of Lisbon
Lisboa, Portugal

Shan Wang
Centre for Marine Technology and Engineering (CENTEC), Instituto Superior Técnico, University of Lisbon
Lisboa, Portugal

C. Guedes Soares
Centre for Marine Technology and Engineering (CENTEC), Instituto Superior Técnico, University of Lisbon
Lisboa, Portugal

ABSTRACT

Quasi-static design of shared mooring systems for floating offshore wind farms is performed in the study using an extended code based on the open-source method MoorPy. It contributes to the baseline design of floating offshore wind farms as part of the ESOMOOR Project. Firstly, the methodology begins with the validation of the in-house MoorPy code with the commercial software DNV SIMA. Then, a static analysis is performed on 14 different multi-body systems across two water depths. This is followed by a quasi-static analysis of the same systems, adding the environmental loads from wind and waves. Various layouts that use multi-segment moorings with fibre ropes are compared. The results focus on key performance indicators, including the tensions at the fairlead (for both anchor lines and shared lines), tensions at the anchor, and the overall system's mean offset.

Keywords: Wind farms, shared mooring, quasi-static analysis, offshore energy.

1. INTRODUCTION

With the rapid expansion of renewable energy, offshore wind turbines have become increasingly prominent in the global energy mix. Compared to onshore installations, offshore wind turbines benefit from higher power generation efficiency due to their larger scale, reduced visual and land-use impacts, and access to stronger and more consistent wind resources.

As offshore wind deployment grows, increased attention has been given to its environmental impacts, particularly on the marine ecosystem. Noise generated during installation and operation has been identified as a primary source of disturbance to marine life [1]. To mitigate seabed impacts, alternative mooring configurations have therefore attracted growing research interest.

For floating offshore platforms and energy devices, extreme wave conditions can induce large motions that generate snap loads in mooring lines, potentially leading to structural damage and reduced system lifespan [2,3]. Consequently, accurate assessment of mooring ultimate loads under survival conditions is critical for the reliable design of floating renewable energy systems. In this context, hybrid mooring systems incorporating synthetic fibre ropes have gained attention due to their economic and operational advantages over conventional chain-based moorings [4–7]. However, commonly used fibre materials, such as polyester, HMPE, and nylon ropes exhibit complex nonlinear mechanical behaviour [8–10], which must be accounted for to ensure accurate prediction of coupled hydrodynamic responses in floating offshore wind turbines (FOWTs) [11] and shallow-water offshore renewable energy devices [12].

Despite these technological advancements, the high cost of offshore wind farm construction and operation remains a key challenge. Offshore projects are particularly capital-intensive due to their distance from consumption centres and the associated grid-connection requirements. As reported by Esteban et al. [13], while the wind turbine itself accounts for approximately 75% of the total cost in onshore projects, this share decreases to about 33% for offshore turbines, highlighting the significant contribution of substructures, moorings, and installation costs.

Previous studies have demonstrated that shared-mooring and shared-anchor configurations offer significant potential for reducing the cost and material demand of floating offshore wind farms (FOWFs) by decreasing the number of mooring lines and anchors per turbine [14, 15]. While these configurations reduce installation and substructure costs, they also introduce stronger hydrodynamic coupling between platforms and alter the overall system dynamics. Numerical and experimental investigations have shown that shared mooring lines reduce mooring restoring stiffness, resulting in increased surge and sway motions and longer natural periods compared to single-turbine systems [16, 17]. Sensitivity and dynamic analyses further indicate that shared-line properties and layout geometry significantly influence restoring forces, mooring tensions, and platform responses, particularly in the horizontal degrees of freedom [18].

Layout optimisation studies highlight the importance of turbine spacing and anchor-line spread angles in achieving efficient mooring designs. While early configurations adopted a 120° spread based on single-turbine layouts, subsequent analyses demonstrated that alternative geometries, such as 90° spreads and polygonal arrays, provide more uniform watch circles and reduce unnecessary stiffness and mooring weight [19]. Different farm layouts were modelled and simulated in SIMA coupled

dynamic analysis software with three and four floaters [20], showing that that designs with two windward legs have significantly lower anchor mooring line tensions than those with a single windward leg, with no relevant variation in platform surge and pitch.

Overall, the existing literature indicates that shared-mooring and shared-anchor concepts offer substantial potential for cost reduction in floating offshore wind farms. Nevertheless, their effective implementation requires careful consideration of hydrodynamic coupling effects, dynamic loading, and layout optimisation under realistic environmental conditions. Within the framework of the ESOMOOR project (www.esomoor.eu), one task addresses the optimisation of shared mooring layouts with synthetic ropes. In this context, the present study provides a preliminary comparative assessment of shared-mooring layouts based on a spar platform with a semi-taut mooring configuration, using the quasi-static mooring analysis tool MoorPy. To enhance economic viability and promote more efficient use of marine space, several multi-body configurations are investigated, enabling the sharing of both mooring lines and anchors among multiple platforms. The maximum fairlead and anchor tensions and the maximum offset for each layout are assessed.

2. METHODOLOGY

The static and quasi-static simulations were performed using the open-source MoorPy code [21], which served as the basis for modelling all single and shared mooring and anchoring systems. In this work, the code is extended to enable the simulation of various shared mooring layouts and shared anchor configurations, allowing flexible analysis of different design scenarios. The theoretical foundation for this approach is detailed by Hall [22].

The MoorPy code uses the quasi-static model, which determines the immediate condition of a mooring line by assuming it is in static equilibrium. The model disregards both hydrodynamic forces and seabed friction, assuming a flat and perfectly horizontal seabed surface. As a result, the tension and weight are the sole forces impacting the suspended section of the mooring line. This means that the only forces considered are the ones related to the net weight and the axial stiffness of the line (EA), the two properties responsible for the line segment characterization.

To determine the shape and tension distribution of a mooring line, a small unstretched segment ds of a free-hanging catenary line is examined. The tension at one end causes an axial strain of T/EA, stretching the element. The weight of the element equals the difference in the vertical tension components at each end. Figure 1 illustrates the conventions used by Hall [22]. The ends of the line, A and B, are identified. The horizontal tension component H is constant over the segment length due to the absence of horizontal forces.

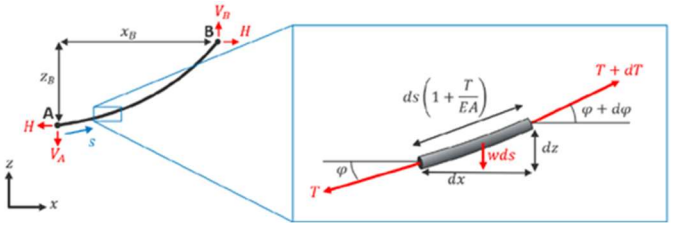

FIGURE 1: DIFFERENTIAL PART OF THE SEGMENT IN MOORPY CALCULATION [22].

Given the uniform material, the quasi-static model is developed based on the following principles: the line segment lies in a vertical plane, allowing for two-dimensional analysis. Only vertical loads apply along the segment length. The horizontal tension component H is uniform and defined as:

$$H = T \cdot \cos\varphi \tag{1}$$

where: T is the total tension; and φ is the local inclination angle. Therefore, the horizontal and vertical coordinates of the profile elements present a typical catenary curve, and they are given by:

$$x(s) = \frac{H}{w}\left\{ ln\left[\frac{V_A + ws}{H} + \sqrt{1 + \left(\frac{V_A + ws}{H}\right)^2}\right] - ln\left[\frac{V_A}{H} + \sqrt{1 + \left(\frac{V_A}{H}\right)^2}\right] \right\} + \frac{Hs}{EA} \tag{2}$$

$$z(s) = \frac{H}{w}\left[\sqrt{1 + \left(\frac{V_A + ws}{H}\right)^2} - \sqrt{1 + \left(\frac{V_A}{H}\right)^2}\right] + \frac{1}{EA}\left(V_A s + \frac{ws^2}{2}\right) \tag{3}$$

To obtain the values of vertical and horizontal tensions, the iterative Newton-Raphson method, stated by Jonkman [23], can be numerically solved using the Jacobian of the positions (J_n) in relation to the tension components:

$$\begin{pmatrix} H_{n+1} \\ V_{B,n+1} \end{pmatrix} = \begin{pmatrix} H_n \\ V_{B,n} \end{pmatrix} - J_n^{-1} \begin{pmatrix} x_{b,n} - x_b^0 \\ z_{b,n} - z_b^0 \end{pmatrix} \tag{4}$$

where n is the iteration number; x_b and z_b are the horizontal and vertical distances between the segment end points, respectively.

Shared-mooring spar systems consist of two different mooring types: the anchored line and the shared line. The anchored line has segments that can behave in three ways: fully suspended, fully resting on the seabed, or partially on the seabed. In contrast, the shared line is entirely suspended, with no contact with the sea bottom. The details on the equations for calculating the line tension and the configuration profile can be found in [20].

In the quasi-static calculations, only the unidirectional mean environmental force from waves and winds are considered. Only the horizontal axis offset is released for the floater and the hydrodynamic and aerodynamic interactions in the farm are neglected.

3. RESULTS AND DISCUSSION

The study investigates a 15-MW wind turbine supported by an innovative spar platform design developed for the ESOMOOR project, analysed at two different sites with water depths of 243.3 meters and 799.2 meters, respectively. The main objective of this model is to compare different layouts for shared mooring systems.

3.1 Design Parameters

The ESOMOOR Project investigates two types of floaters: a semisubmersible and a spar. However, in the present study, only the spar platform is examined. As mentioned previously, the spar platform experiences reduced wave effects due to its small waterplane area, and therefore, it is well suited for deep-water applications. The spar platform has a draft of 110 meters and a freeboard of 15 meters. The FOWT configuration is illustrated in Figure 2, and the main floater parameters are presented in Table 1. The wind turbine has a power rating of 15 MW and is based on the IEA-15 MW project [25].

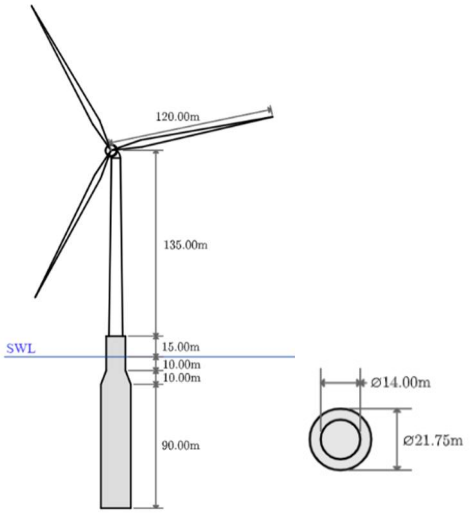

FIGURE 2: ESOMOOR'S SPAR PLATFORM REPRESENTATION [24].

TABLE 1: PROPERTIES OF THE ESOMOOR'S SPAR PLATFORM.

Parameter	Value	Unit
Depth to platform base below SWL	110.00	m
Freeboard	15.00	m
Depth to top and bottom of taper below SWL	10.00, 20.00	m
Platform diameter above and below taper	14.00, 21.75	m
Platform mass	35,917.00	t
CM height	-79.30	m

3.2 Mooring Lines

The anchor lines consist of a multi-segment mooring, with chain at both the top and bottom sections, connecting the anchor to the fairlead, and polyester in the middle section. Initially, they are arranged in a semi-taut configuration, ensuring that the fibre portion does not touch the seabed for safety. The shared lines are made entirely of polyester and are set to a length equal to 1200 meters. The mooring configuration is illustrated in Figure 3.

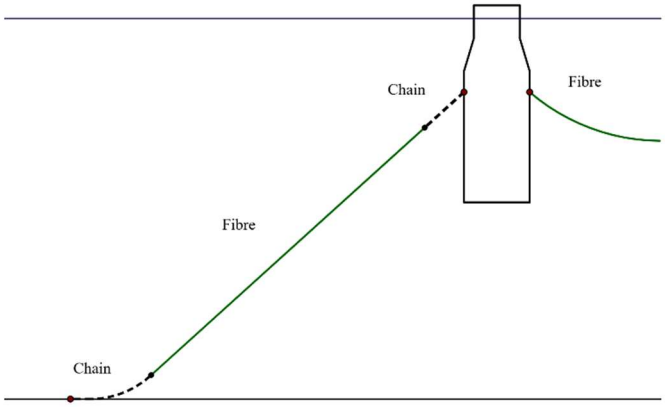

FIGURE 3: MULTI-SEGMENT MOORING REPRESENTATION [24].

TABLE 2: MOORING MAIN PARAMETERS.

Parameter		EU	USA	Unit
Water depth		243.30	799.20	m
Shared line length		1200.00	1200.00	m
Anchor radius		925.00	2100.00	m
Anchor line total length		950	2250	m
	Length	870.00	2100.00	m
	Diameter	170.00	170.00	mm
Polyester	Axial stiffness	1.21E+08	1.21E+08	N/m
	Weight	4.75	4.75	kg/m
	Breaking strength	8.64E+06	8.64E+06	N
	Length (bottom)	50.00	100.00	m
	Length (top)	30.00	50.00	m
	Diameter	110.00	110.00	mm
Chain	Axial stiffness	1.04E+09	1.04E+09	N/m
	Weight	242.00	242.00	kg/m
	Breaking strength	1.17E+07	1.17E+07	N

The study investigates two locations: one in the European Union, with a water depth of 243.3 meters, and the other on the USA coast, where the water depth is greater, at 799.2 meters. The mooring parameters vary depending on the water depth, and the values used are estimations for an initial semi-taut configuration. The polyester properties were obtained from an internal catalogue provided by a project partner mooring company, while the chain properties are based on the R4 studless chain. The mooring properties are detailed in Table 2.

3.3 Environmental Parameters

The environmental parameters are defined under extreme conditions, where the turbine blades are parked because the wind speed exceeds the cut-out threshold. As only static and quasi-static analyses are considered, the primary focus is on the forces applied to the system. The ESOMOOR project defines these forces based on the 50-year return period for both locations. The

wind-induced forces on the tower are defined using Frøya, while those on the blades are obtained through SIMA. As in the first case study, all forces are applied along the x-axis. The environmental properties are detailed in Table 3.

TABLE 3: ENVIRONMENTAL PARAMETERS.

Parameter		EU	USA	Unit
Condition	H_s	15.7	12.2	m
	T_p	16.7	14.6	s
	U_{hub}	40.4	39.1	m/s
Loads	Wind (tower)	840.0	790.0	kN
	Wind (blades)	510.0	510.0	kN
	Mean wave drift	6.5	4.9	kN

3.4 System Layouts

In total, 15 systems were modelled in MoorPy in the study. The first model represents a single spar, used exclusively to validate the platform properties and the multi-segment anchor line. In addition, 14 shared mooring layouts were created, ranging from configurations with two turbines up to ten turbines. The developed designs are shown in Table 4. For the layouts with six, eight, nine, and ten wind turbines, two different configurations were modelled, one using a single anchor line and the other using two anchor lines on the two upstream and two downstream turbines. The distance between spars, where lines are shared, is equal to five times the rotor diameter (1200 meters).

TABLE 4: WIND FARM MODELLED LAYOUTS.

Layout	Description	Wind Turbines	Anchors	Shared Lines	Mooring Angle*	Representation
L1	Single	1	3	0	0º, 60º	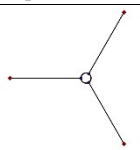
L2	Dual	2	4	1	60º	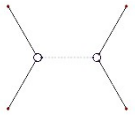
L3.1	Tandem	3	6	2	60º	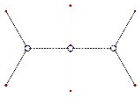
L3.2	Staggered	3	3	3	0º, 60º	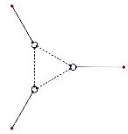
L4.1	Diamond	4	4	4	0º, 90º	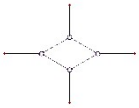
L4.2	2x2	4	4	4	45º	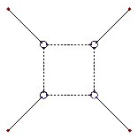
L6.1	Hexagonal	6	6	6	0º, 60º	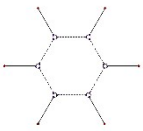
L6.2	2x3	6	6	7	45º, 90º	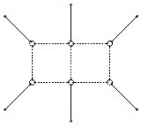

L6.3	2x3	6	10	7	0º, 90º	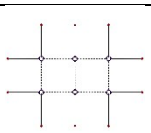
L8.1	2x4	8	8	10	45º, 90º	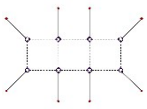
L8.2	2x4	8	12	10	0º, 90º	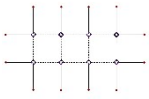
L9.1	3x3	9	8	12	0º, 45º, 90º	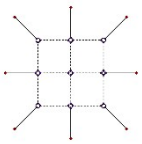
L9.2	3x3	9	12	12	0º, 90º	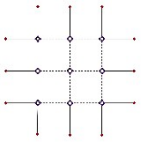
L10.1	2x5	10	10	13	45º, 90º	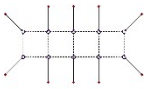
L10.2	2x5	10	14	13	0º, 90º	

*Anchor line angle relative to environmental loads (x-axis).

4. RESULTS AND DISCUSSION

4.1 Code Validation

To validate the MoorPy code, particularly the spar floater parameters and mooring properties, the static and quasi-static results for the single-spar system were compared with those from the equivalent SIMA model. Different from the previous case study, this system uses a multi-segmented mooring line, requiring new validation. For this purpose, the single-spar layout (L1) was used. In addition, the dual-spar layout (L2) was tested to validate the shared mooring model and the platform's restoring coefficients.

The mooring properties used in the validation process were obtained from the ESOMOOR Project through an optimisation procedure with the objective of minimising mooring costs for a single-spar system. The general system parameters used in this section are the same as those presented in Table 4, except for the modifications listed in Table 5.

The first validation test was a static analysis of the single-spar system. This test aimed to compare the tensions along the anchor line and verify whether the multi-segmented mooring, composed of chain–polyester–chain sections, was modelled correctly. The results are presented in Table 6.

TABLE 5: OPTIMISED MOORING PROPERTIES FOR CODE VALIDATION.

Parameter		EU	Unit
Anchor radius		705.1	m
Anchor line total length		729.9	m
Polyester	Length	583.9	m
Chain	Length (bottom)	116.0	m
	Length (top)	30.0	m

TABLE 6: STATIC ANALYSIS CODE VALIDATION FOR SINGLE-SPAR.

Point	MoorPy	SIMA	Diff.
Fairlead Tension	390.18 kN	388.82 kN	0.35 %
Anchor Tension	332.45 kN	332.76 kN	0.09 %

TABLE 7: QUASI-STATIC ANALYSIS CODE VALIDATION FOR SINGLE-SPAR.

Parameter		MoorPy	SIMA	Diff.
Fairlead	Max.	1568.78 kN	1566.50 kN	0.15%
Tension	Min.	166.99 kN	163.93 kN	1.83%
Anchor	Max.	1476.55 kN	1477.40 kN	0.06%
Tension	Min.	112.08 kN	109.95 kN	1.90%
Mean Offset	WT1	10.74 m	10.73 m	0.08%

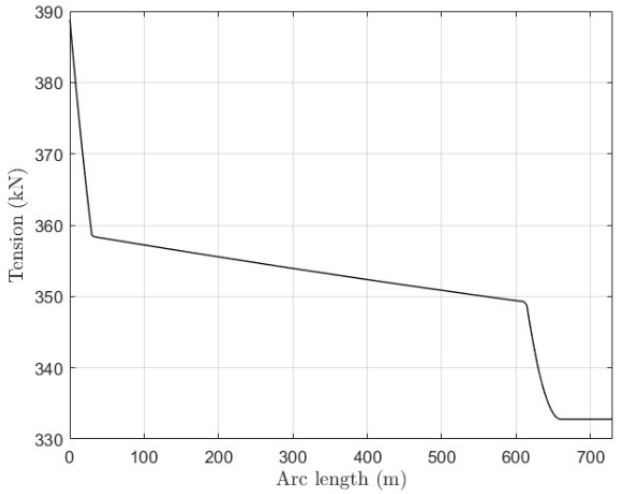

FIGURE 4: SIMA SINGLE-SPAR SYSTEM: STATIC DISTRIBUTION ALONG THE ANCHOR LINE.

As shown in Table 6, the results from the MoorPy code and SIMA differ by less than 0.35%, showing very good agreement. Although both methods model the mooring properties differently, these results indicate that the properties were represented consistently. Furthermore, Figure 4 shows that the tension distribution from SIMA follows a semi-taut configuration, where only part of the bottom chain experiences the same tension as the anchor.

Next, a quasi-static analysis is performed for the same system to validate the FOWT response under mean environmental forces. The results are presented in Table 7. After applying the external forces, the results showed a slightly larger difference between the MoorPy and SIMA values; however, this difference remains small and acceptable for this test. The mean platform offset also presented a very small deviation of only 0.08%. Figure 5 illustrates the tension distribution in the upstream anchor line, where the tension is higher, and in the downstream lines, where it is lower.

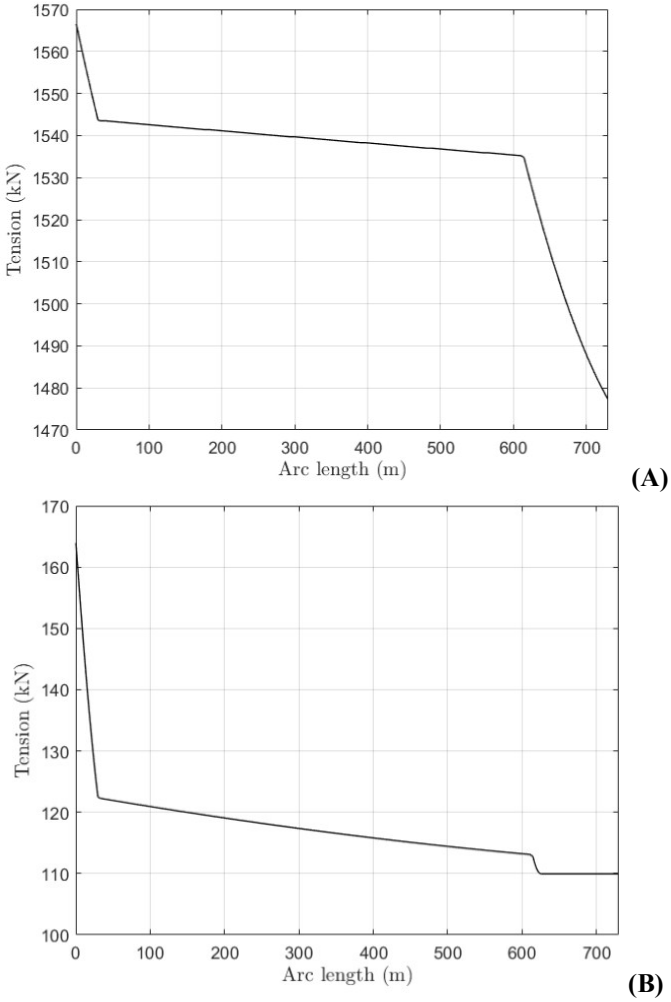

FIGURE 5: SIMA SINGLE-SPAR SYSTEM: QUASI-STATIC TENSION DISTRIBUTION ALONG THE **(A)** UPSTREAM ANCHOR LINE; **(B)** DOWNSTREAM ANCHOR LINE.

Figure 6 presents the MoorPy plot of the system, where the grey lines represent the static configuration and the purple lines show the mooring arrangement after the forces are applied. Additionally, the SIMA plot is included, indicating the mean offset obtained. The second validation test involves a dual-spar system with a shared mooring line. First, a static analysis was performed to verify whether the shared line is modelled correctly and to assess whether adding a second body affects the results between the two methods. The static analysis results are presented in Table 8, and the tension distribution along the system's anchor and shared lines is shown in Figure 7.

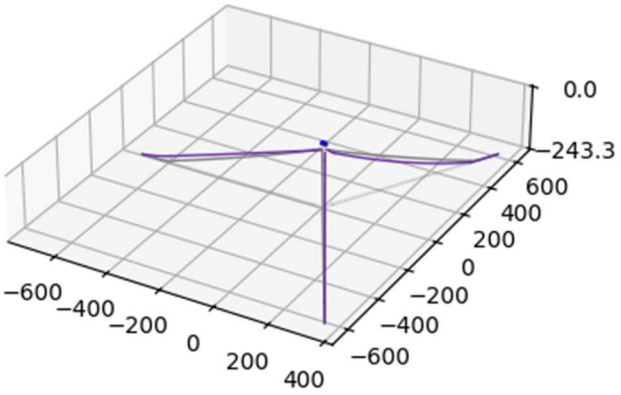

(A)

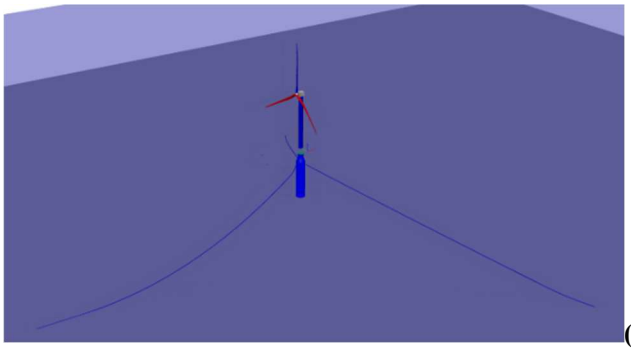

(B)

FIGURE 6: SINGLE-SPAR QUASI-STATIC RESULT IN **(A)** MOORPY; **(B)** SIMA.

TABLE 8: STATIC ANALYSIS CODE VALIDATION FOR DUAL-SPAR.

Point	MoorPy	SIMA	Diff.
Fairlead Tension (Anchor Line)	192.82 kN	188.94 kN	2.01%
Anchor tension	137.33 kN	136.00 kN	0.97%
Fairlead Tension (Shared Line)	137.73 kN	136.41 kN	0.96%
Initial Displacement	8.45 m	8.35 m	1.18%

TABLE 9: QUASI-STATIC ANALYSIS CODE VALIDATION FOR DUAL-SPAR.

Parameter		MoorPy	SIMA	Diff.
Fairlead Tension (Anchor Line)	Max.	2705.89 kN	2704.90 kN	0.04%
	Min.	97.01 kN	93.79 kN	3.32%
Anchor Tension	Max.	2607.42 kN	2609.40 kN	0.08%
	Min.	24.41 kN	24.19 kN	0.90%
Fairlead Tension (Shared Line)		1377.04 kN	1377.00 kN	0.00%
Mean Offset	WT1	33.37 m	33.32 m	0.15%
	WT2	70.95 m	70.89 m	0.08%

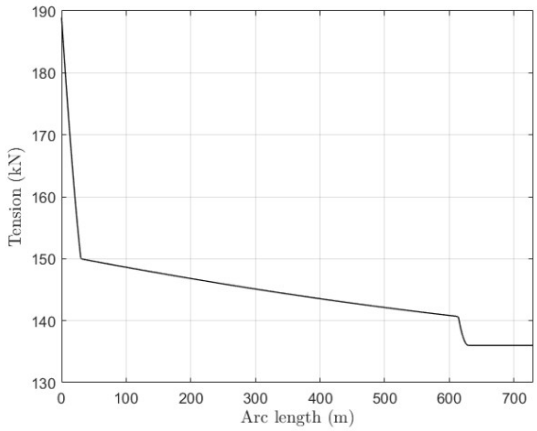

(A)

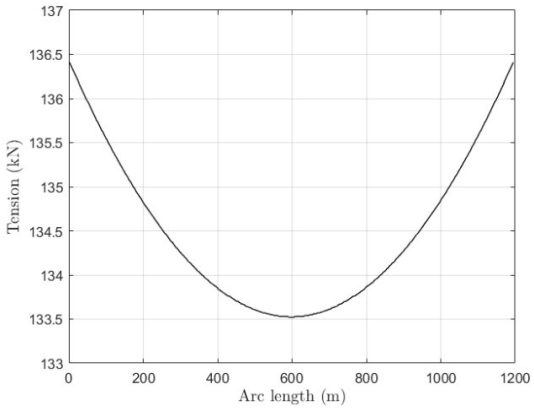

(B)

FIGURE 7: SIMA DUAL-SPAR SYSTEM: STATIC TENSION DISTRIBUTION ALONG THE **(A)** ANCHOR LINE; **(B)** SHARED LINE.

Overall, the results are very similar, with the largest difference observed at the anchor line fairlead, which remains within acceptable limits. The initial displacement (equilibrium position) differs by only 0.1 meters. The static distribution indicates that the configuration is still semi-taut, although a large portion of the bottom chain is already in contact with the seabed. The shared line presents a parabolic tension distribution with minimal variation, as expected.

Finally, a quasi-static test was performed on the dual-spar system to evaluate whether the platforms exhibit the same stiffness and whether the system maintains a semi-taut configuration under the mean environmental forces using these optimised values. The results of the test are presented in Table 9.

The validation process is thus completed, showing good agreement in the final test as well. The largest difference was observed in the tension at the downstream fairlead, where the system no longer exhibits a semi-taut configuration (Figure 8). This indicates that part of the polyester section experiences the same tension as the anchor, meaning that it is in contact with the seabed. Consequently, the optimised values for the single-spar system cannot be applied to the dual-spar system.

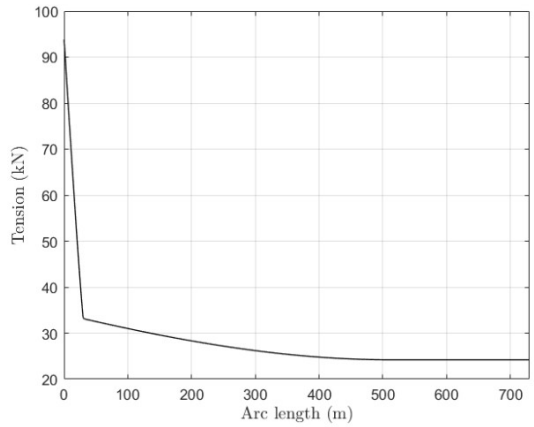

FIGURE 8: SIMA DUAL-SPAR SYSTEM: QUASI-STATIC TENSION DISTRIBUTION ALONG THE DOWNSTREAM ANCHOR LINE

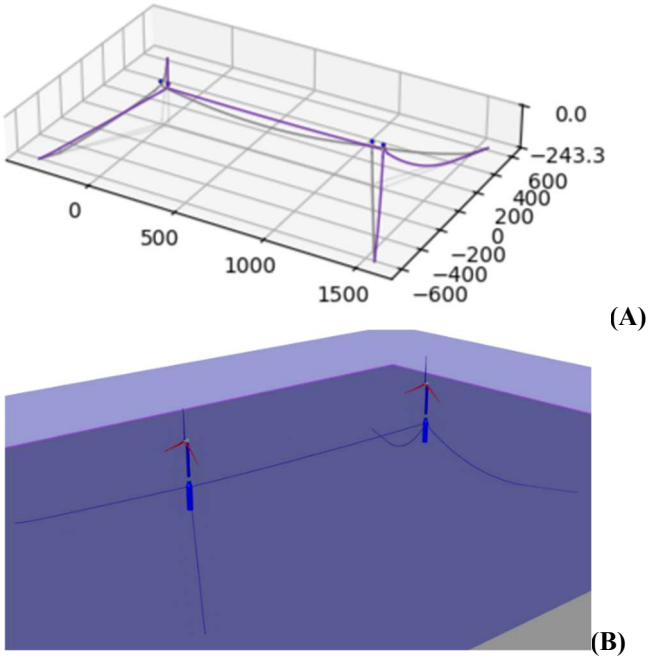

FIGURE 9: DUAL-SPAR QUASI-STATIC RESULT REPRESENTATION IN **(A)** MOORPY; **(B)** SIMA.

The MoorPy static and quasi-static plots for the dual-spar system are shown in Figure 9, alongside the SIMA model after displacement. It is noticeable that the downstream turbines adopt more of a catenary configuration rather than a semi-taut one, with a large portion of the mooring in contact with the seabed. This should not occur, as the polyester is not designed to touch the seabed and could be damaged or even break if it does.

4.2 Static Analysis

The static results are first presented in two summary tables: one for the European shore (Table 10) and another for the American shore (Table 11). The values are then discussed in detail for each layout. The analysis focuses on fairlead tensions in the anchor and shared lines, as well as the tension at the anchor points. All 14 shared systems were tested. Due to differences in the z-displacement of each wind turbine, the tensions show minor variations; in this section, only the maximum tension is listed.

The first layouts tested are the dual- and three-spar systems. Layouts L2 and L3.1 share a similar geometry, with the wind turbines arranged in tandem, while L3.1 and L3.2 contain the same number of FOWTs. In both cases, it is evident that tensions in the anchor line, at the fairleads, and at the anchor points increase when an additional wind turbine is added. However, the shared line of the three-spar system, given its defined length, exhibits lower tension. Comparing L3.1 and L3.2, the static analysis indicates that in deep waters, the staggered configuration tends to present lower tension than the tandem arrangement.

TABLE 10: STATIC RESULTS IN EUROPEAN LOCATION.

Layout	Fairlead Tension [kN]		Anchor Tension [kN]
	Anchor Line	Shared Line	
L1	141.8	-	86.6
L2	139.5	87.9	83.5
L3.1	142.3	86.3	86.9
L3.2	166.6	72.5	115.8
L4.1	175.2	78.0	125.8
L4.2	154.1	77.0	101.4
L6.1	136.8	84.9	81.2
L6.2	155.6	86.3	103.4
L6.3	138.1	86.4	82.8
L8.1	156.5	86.4	104.4
L8.2	138.1	86.4	82.8
L9.1	156.4	84.8	104.3
L9.2	137.0	93.2	81.7
L10.1	157.1	86.4	105.1
L10.2	138.1	86.4	82.8

TABLE 11: STATIC RESULTS IN AMERICAN LOCATION.

Layout	Fairlead Tension [kN]		Anchor Tension [kN]
	Anchor Line	Shared Line	
L1	310.7	-	194.2
L2	293.8	176.3	175.5
L3.1	311.1	162.0	194.6
L3.2	292.2	104.1	173.6
L4.1	318.2	121.4	201.8
L4.2	282.2	118.1	162.3
L6.1	265.8	145.8	143.2
L6.2	281.6	163.4	161.7
L6.3	281.6	163.4	161.8
L8.1	281.6	163.7	160.4
L8.2	281.8	164.0	161.9
L9.1	269.6	144.9	147.2
L9.2	276.0	156.5	154.3
L10.1	281.7	163.7	161.7
L10.2	282.0	164.1	162.1

At water depths of 243.3 meters and 799.2 meters, for Layouts L4.1 and L4.2, the tensions at the fairleads and anchor points are lower for the diamond configuration layout. It is also noticeable that tensions are more evenly distributed in the 2x2 layout, where the symmetrical arrangement may offer an advantage.

Layouts L6.1, L6.2, and L6.3 each feature six floating wind turbines. The hexagonal configuration exhibits the lowest tension among these layouts, as its symmetrical design and multiple shared lines result in equal tension across all anchor lines. Layout L6.3 includes four more anchor lines than L6.2, leading to lower tensions at all points in the European site. However, in the deeper waters of the United States, tensions become similar for both layouts.

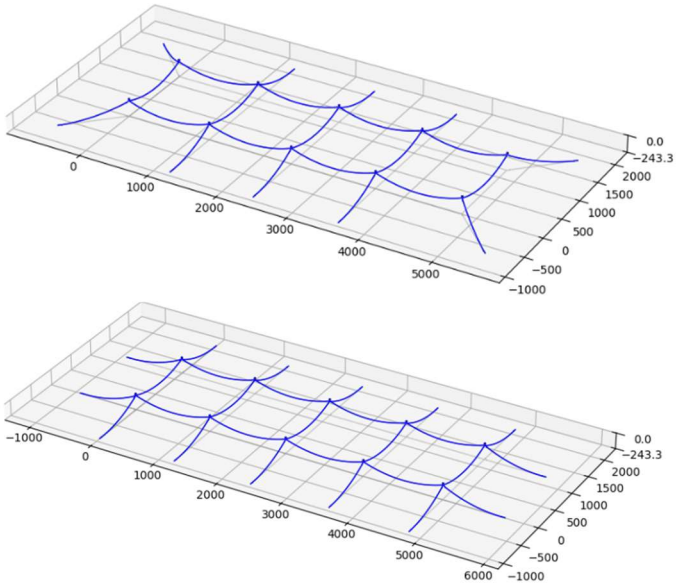

FIGURE 10: STATIC CONFIGURATION IN EU FOR **(A)** L10.1; **(B)** L10.2.

Similar to layouts L6.2 and L6.3, layouts L8.1 and L8.2, the tension behaviour varies with water depth. At shallower depths, the layout with fewer anchor lines exhibits higher tension at the fairleads and anchor points, whereas in deeper waters the tensions are more similar. The layout with nine wind turbines features a 3x3 arrangement. The difference between layouts L9.1 and L9.2 lies in the number of anchor lines on the floaters connected to only two other spars. In shallower waters, L9.1 exhibits higher tension in the anchor lines than L9.2, whereas in the American site this behaviour is reversed. In both locations, the shared line tension for L9.2 is slightly higher.

Finally, the layouts with ten wind turbines feature a 2x5 configuration, with the same difference in anchor lines as observed for L9.1 and L9.2. The results are shown in Figure 10. The static behaviour follows the same pattern observed in all layouts where additional anchor lines are introduced: tension values tend to converge in deeper waters.

4.3 Quasi-static Analysis

The quasi-static analysis is divided into two parts: tension and mean offset. For the tension analysis, the code was developed to verify whether the maximum tension at all points along the mooring are below the minimum breaking load with the safety factor of 1.7. The results are presented in Tables 12, 13, 14 and 15.

For both locations, layout L6.1, with a hexagonal arrangement, did not converge in the quasi-static simulations. After applying the forces, the offset became too large, preventing the algorithm from calculating the tensions. The upstream wind turbine experiences excessive tension and cannot restore the system; therefore, this layout must be disregarded. Layouts with eight turbines, L8.1 and L8.2, exhibited the same issue, but only at the European site, where the water depth is lower.

TABLE 12: QUASI-STATIC TENSION RESULTS FOR FOWFS IN EUROPEAN LOCATION.

Layout	Fairlead Tension [kN]				Anchor Tension [kN]		Integrity Check
	Anchor Line		Shared Line				
	Max.	Min.	Max.	Min.	Max.	Min.	
L1	1469.9	116.5	-	-	1421.1	1108.2	PASS
L2	2587.5	92.1	1370.6	1370.6	2535.3	16.7	PASS
L3.1	3728.2	86.3	2671.4	1362.3	3678.2	7.9	PASS
L3.2	3562.3	83.3	2380.7	788.3	3514.0	1.4	PASS
L4.1	5253.8	81.7	2121.2	771.3	5203.9	0.5	ERROR
L4.2	3708.7	87.5	2306.1	57.6	3658.3	9.3	PASS
L6.1	-	-	-	-	-	-	ERROR
L6.2	5429.1	85.4	3328.1	49.5	5379.1	3.6	ERROR
L6.3	4168.0	82.1	2689.5	87.0	4119.0	1.3	PASS
L8.1, L8.2	-	-	-	-	-	-	ERROR
L9.1	5081.3	82.8	2969.6	59.0	5046.2	1.2	PASS
L9.2	4196.5	81.2	2714.3	84.8	4147.5	1.3	PASS
L10.1	7760.5	80.1	4615.2	262.4	7710.5	4.7	ERROR
L10.2	6382.8	81.2	4844.9	89.7	6317.7	0.0	ERROR

TABLE 13: QUASI-STATIC DISPLACEMENT RESULTS FOR FOWFS IN EUROPEAN LOCATION.

Layout	Offset [m]									
	WT1	WT2	WT3	WT4	WT5	WT6	WT7	WT8	WT9	WT10
L1	22.3	-	-	-	-	-	-	-	-	-
L2	60.6	94.5	-	-	-	-	-	-	-	-
L3.1	77.1	125.0	159.8	-	-	-	-	-	-	-
L3.2	103.8	103.8	133.1	-	-	-	-	-	-	-
L4.1	45.3	110.6	110.6	160.4	-	-	-	-	-	-
L4.2	73.2	73.2	113.6	113.6	-	-	-	-	-	-
L6.2	93.7	146.8	186.4	93.7	146.8	186.4	-	-	-	-
L6.3	44.4	93.2	128.6	44.4	93.2	128.6	-	-	-	-
L6.1, L8.1,L8.2	-	-	-	-	-	-	-	-	-	-
L9.1	109.7	161.8	200.4	47.1	96.5	132.1	109.7	161.8	200.4	-
L9.2	44.4	93.2	128.6	44.6	93.6	129.2	44.4	93.2	128.6	-
L10.1	120.6	191.3	249.0	295.5	333.9	120.6	191.3	249.0	295.5	333.9
L10.2	61.2	132.1	189.8	234.4	266.8	61.2	132.1	189.8	234.4	266.8

TABLE 14: QUASI-STATIC TENSION RESULTS FOR FOWFS IN AMERICAN LOCATION.

Layout	Fairlead Tension [kN]				Anchor Tension [kN]		Integrity Check
	Anchor Line		Shared Line				
	Max.	Min.	Max.	Min.	Max.	Min.	
L1	1597.3	254.7	-	-	1449.3	309.6	PASS
L2	2657.2	210.5	1368.8	1368.8	2513.9	73.5	PASS
L3.1	3758.6	195.3	2593.8	1347.5	3612.6	53.4	PASS
L3.2	3697.4	172.6	2414.5	770.2	3551.9	21.9	PASS
L4.1	5361.4	170.4	2071.6	743.6	5215.8	18.7	ERROR
L4.2	3821.5	192.7	2328.4	1338.3	3676.3	49.9	PASS
L6.1	-	-	-	-	-	-	ERROR
L6.2	5532.1	179.3	3342.7	59.1	5386.4	32.2	ERROR
L6.3	4204.7	178.0	2610.6	155.8	4147.1	30.3	PASS
L8.1	7159.1	170.0	4252.5	55.8	7015.5	20.2	ERROR
L8.2	5520.6	166.1	3860.4	155.9	5375.1	15.8	ERROR
L9.1	5132.9	175.8	3037.2	68.3	4987.2	27.7	ERROR
L9.2	4243.6	177.7	2639.4	130.8	4097.8	30.0	PASS
L10.1	8549.8	164.1	5006.4	54.8	8408.4	314.3	ERROR
L10.2	6781.0	159.2	5063.2	157.3	6637.3	7.5	ERROR

TABLE 15: QUASI-STATIC DISPLACEMENT RESULTS FOR FOWFS IN AMERICAN LOCATION.

Layout	Offset [m]									
	WT1	WT2	WT3	WT4	WT5	WT6	WT7	WT8	WT9	WT10
L1	51.8	-	-	-	-	-	-	-	-	-
L2	149.2	166.0	-	-	-	-	-	-	-	-
L3.1	196.4	226.5	244.2	-	-	-	-	-	-	-
L3.2	211.9	211.9	225.6	-	-	-	-	-	-	-
L4.1	121.9	195.2	195.2	253.4	-	-	-	-	-	-
L4.2	159.0	159.0	182.2	182.2	-	-	-	-	-	-
L6.2	211.5	248.9	273.4	211.5	248.9	273.4	-	-	-	-
L6.3	119.6	151.6	170.8	119.6	151.6	170.8	-	-	-	-
L8.1	259.4	310.2	348.6	374.1	259.4	310.2	348.6	374.1	-	-
L8.2	150.7	196.7	230.0	250.4	150.7	196.7	230.0	250.4	-	-
L9.1	219.3	257.3	282.5	130.4	163.1	182.5	219.3	257.3	282.5	-
L9.2	119.7	151.7	170.8	120.4	152.6	171.8	119.7	151.7	170.8	-
L10.1	299.7	362.0	412.4	450.7	477.0	299.7	362.0	412.4	450.7	477.0
L10.2	179.5	238.8	285.5	319.6	340.9	179.5	238.8	285.5	319.6	340.9

The shared mooring in layout L2 exhibits a similar tension to the downstream shared line in L3.1, but with generally much lower offset displacements. Comparing L3.1 and L3.2, the triangular staggered configuration results in lower tensions at the fairleads for both the anchor and shared lines. The mean offset is more evenly distributed, with WT1 slightly higher, while all wind turbines display similar displacements. This indicates a more unified system, with consistent behaviour among the floaters.

Layout L4.1 exhibits very high tension at the upstream anchor line, as it is aligned with the environmental forces in this test. This results in tensions reaching 5253.8 kN in Europe and 5361.4 kN in the American site, causing the layout to fail the integrity check with a safety factor of 1.7 in both locations. Layout L4.2 shows a better-distributed tension, as the two upstream wind turbines share the pulling force, and it also presents a lower maximum offset.

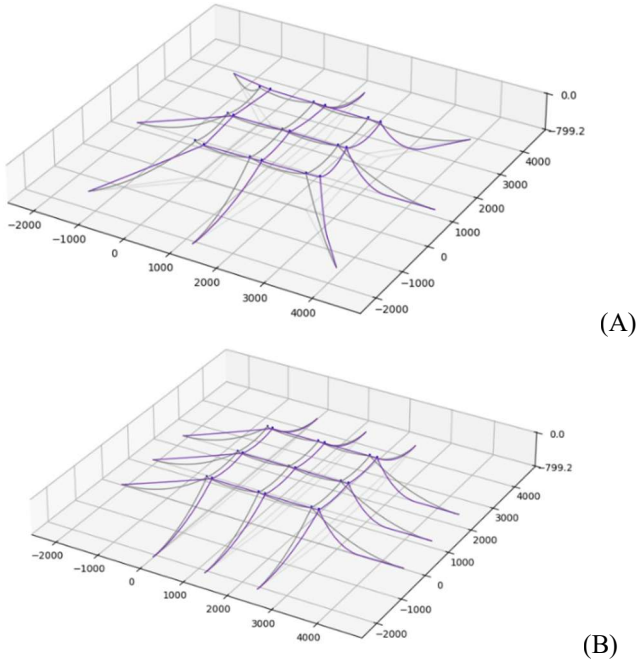

(A)

(B)

FIGURE 11: QUASI-STATIC CONFIGURATION IN USA FOR **(A)** L9.1; **(B)** L9.2.

The first layout with six wind turbines did not produce convergent results in the code calculations. As a result, tension values were obtained only for layouts L6.2 and L6.3. Both layouts show similar maximum tensions at the fairleads and anchor points. With the addition of another anchor line in layout L6.3, the maximum tension decreases by about 1300 kN. Hence, only this layout passed the tension integrity check, while L6.1 remains vulnerable under extreme environmental conditions. For L6.3, the offset is also lower, with WT1 showing nearly half the displacement of WT1 in L6.2.

For the 8-wind turbine layouts, results converged only in deeper waters, so data are available only for the American site. Even with converged values, neither layout passed the tension integrity check. For layout L8.1, tensions at the upstream turbines, WT1 and WT5, reach 7159.1 kN, close to the MBL of the polyester. Layout L8.2 shows the expected effect of adding a new anchor line: the tension is more evenly distributed, but still high enough to be vulnerable under extreme conditions. Notably, the fairlead at the shared line between WT1 and WT5 exhibits the highest tension among all shared lines in L8.1, whereas it has the lowest tension in L8.2. This demonstrates that adding a new anchor line for these turbines immediately reduces the tension in the shared lines separating them. The mean offsets of the systems are also significant, with the downstream wind turbine reaching 46.8\% of the water depth in L8.1 and 31.3% in L8.2.

The plots for layouts L9.1 and L9.2 are shown in Figure 11, respectively. At a water depth of 243.3 meters, both layouts passed the integrity check; however, at 799.2 meters, layout L9.1 exhibits tensions exceeding the allowable limit.

5 CONCLUSION

This study investigates the performance of offshore floating wind farms employing shared mooring lines by examining the quasi-static response of 15-MW wind turbine systems under various mooring layouts and configurations. Fourteen different layouts are modelled in MoorPy and the tensions on the fairleads and anchors and the maximum offsets are compared.

Results reveal that configurations with a single main upstream turbine, such as the four-spar diamond and six-spar hexagonal shapes, concentrate excessive tension on the upstream floater's fairleads, making them unsuitable for extreme sea states. However, adding an additional anchor line to platforms connected to only two others proved highly beneficial, reducing fairlead tensions by more than 1000 kN and lowering mean offsets by up to 50% in several cases. These results highlight the importance of distributing loads efficiently across the array to maintain structural integrity in large-scale shared-line systems.

Future work should focus on optimising array layouts by accounting for different mooring materials, mooring-line lengths, and platform spacing. In addition, the inclusion of electrical umbilicals is necessary to better capture the overall system stiffness. The use of buoys along shared mooring lines should also be investigated to explore additional strategies for mitigating peak tensions at connection points. Finally, the present study is limited to quasi-static analyses assuming unidirectional environmental loading and surge motion only. Fully coupled dynamic analyses under ultimate (ULS), accidental (ALS), and fatigue (FLS) limit states are therefore required to comprehensively assess and confirm the proposed mooring designs.

ACKNOWLEDGEMENTS

This work has been supported by the project "Enhancing shared mooring system design for floating offshore wind farms (ESOMOOR)", funded by the Fundação para a Ciência e Tecnologia with the project reference CETP/0002/2023, and co-funded by the European Union, with the project reference CETP-2023-00145. However, the views and opinions expressed are those of the author(s) only and do not necessarily reflect those of the European Union or the CETPartnership. Neither the

European Union nor the granting authority can be held responsible for them.

The authors would also like to acknowledge BEXCO for providing the properties of the synthetic ropes used in this study. In addition, this work was carried out within the framework of the Strategic Research Plan of the Centre for Marine Technology and Ocean Engineering (CENTEC), financed by the Portuguese Foundation for Science and Technology (FCT) under contract UID/00134/2025 (https://doi.org/10.54499/UID/00134/2025).

REFERENCES

[1] Bailey, H., Brookes, K. L., and Thompson, P. M., 2014, "Assessing Environmental Impacts of Offshore Wind Farms: Lessons Learned and Recommendations for the Future," Aquatic Biosystems, Vol. 10, pp. 1–13.

[2] Hsu, W.-T., Thiagarajan, K. P., and Manuel, L., 2017, "Extreme Mooring Tensions Due to Snap Loads on a Floating Offshore Wind Turbine System," Marine Structures, Vol. 55, pp. 182–199.

[3] Kvitrud, A., 2014, "Lessons Learned from Norwegian Mooring Line Failures 2010–2013," Proc. ASME 2014 33rd International Conference on Ocean, Offshore and Arctic Engineering (OMAE2014), San Francisco, CA, USA, Paper No. OMAE2014-23474.

[4] Xu, S., Wang, S., and Guedes Soares, C., 2019, "Review of Mooring Design for Floating Wave Energy Converters," Renewable and Sustainable Energy Reviews, Vol. 111, pp. 595–621.

[5] Xu, S., Wang, S., and Guedes Soares, C., 2021, "Experimental Study of the Influence of the Rope Material on Mooring Fatigue Damage and Point Absorber Response," Ocean Engineering, Vol. 232, p. 108667.

[6] Lin, T.H., and Yang, R.Y., 2023, "Stability Analysis and Environmental Influence Evaluation on a Hybrid Mooring System for a Floating Offshore Wind Turbine," Journal of Marine Science and Engineering, Vol. 11, No. 12, p. 2236.

[7] Lian Y, Zhong F, Zheng J, Chen W, Ma G, Wang S, Yim SC., 2023, "Effects of Mooring Lines with Different Materials on the Dynamic Response of Offshore Floating Wind Turbines," Journal of Marine Science and Engineering, Vol. 11, No. 12, p. 2302.

[8] Xu, S., Wang, S., Liu, H., Zhang, Y., Li, L., and Guedes Soares, C., 2021, "Experimental Evaluation of the Dynamic Stiffness of Synthetic Fibre Mooring Ropes," Applied Ocean Research, Vol. 112, p. 102709.

[9] Lian, Y., Liu, H., Zhang, Y., and Li, L., 2017, "An Experimental Investigation on Fatigue Behaviors of HMPE Ropes," Ocean Engineering, Vol. 139, pp. 237–249.

[10] Feng, L., Wang, Q., Wang, S., and Xu, S., 2024, "Experimental Characterization of Stiffness of a Polyester Mooring Rope for a CFP SO," Journal of Marine Science and Engineering, Vol. 12, No. 8, p. 1435.

[11] Pham, H.D., Cartraud, P., Schoefs, F., Soulard, T., and Berhault, C., 2019, "Dynamic Modeling of Nylon Mooring Lines for a Floating Wind Turbine," Applied Ocean Research, Vol. 87, pp. 1–8.

[12] Depalo, F., Wang, S., Xu, S., Guedes Soares, C., Yang, S.H., and Ringsberg, J. W., 2022, "Effects of Dynamic Axial Stiffness of Elastic Moorings for a Wave Energy Converter," Ocean Engineering, Vol. 251, p. 111132.

[13] Esteban, M. D., Diez, J. J., López, J. S., and Negro, V., 2011, "Why Offshore Wind Energy?" Renewable Energy, Vol. 36, No. 2, pp. 444–450.

[14] Sloan, C., Hall, M.; Housner, S., Lozon, E., Sirnivas, S., 2022, "Shared Mooring Systems for Deep-Water Floating Wind Farms," Technical Report NYSERDA Contract 142869.

[15] Striani, R., Jiang, H., Biroli, M.V., Shao, Y. and Wang, S., 2025, "Review of Floating Offshore Wind Turbines with Shared Mooring Systems," Journal of Marine Science and Engineering, 13(12), p.2341.

[16] Munir, H., Lee, C.F. and Ong, M.C., 2021, "Global analysis of floating offshore wind turbines with shared mooring system," In IOP Conference Series: Materials Science and Engineering (Vol. 1201, No. 1, p. 012024). IOP Publishing.

[17] Lopez-Olocco, T., Liang, G., Medina-Manuel, A., Ynocente, L.S., Jiang, Z. and Souto-Iglesias, A., 2023. Experimental comparison of a dual-spar floating wind farm with shared mooring against a single floating wind turbine under wave conditions. Engineering Structures, 292, p.116475.

[18] Liang, G. Jiang, Z. and Merz. K., 2023, "Dynamic analysis of a dual-spar floating offshore wind farm with shared moorings in extreme environmental conditions. Marine Structures," 90:103441, 2023.

[19] Wilson, S., Hall, M., Housner, S. and Sirnivas, S., 2021, "Linearized modeling and optimization of shared mooring systems," Ocean Engineering, 241, p.110009.

[20] Biroli, M.V., Vidal, F.J., Desiderati, J., Wang, S. and Guedes Soares, C., 2025, "Dynamic Analysis of Shared Moorings in Different Wind Farm Layouts," Marine Energy Research, 2(3), p.10012.

[21] Hall, M., Housner, S., Sirnivas, S. and Wilson, S., 2021. Moorpy (quasi-static mooring analysis in python) (No. MoorPy). National Renewable Energy Laboratory (NREL), Golden, CO (United States).

[22] Hall, M., 2024, "Generalized quasi-static mooring system modeling with analytic Jacobians," Energies, 17(13), p.3155.

[23] Jonkman, J.M., 2007, "Dynamics modeling and loads analysis of an offshore floating wind turbine," University of Colorado at Boulder.

[24] Striani, R; Biroli, M; Wang, S., 2025, "ESOMOOR D3.1: Definition of two floaters for IEA 15WM turbine for at least two water depths in Europe and the US," Technical University of Denmark. Online resource. https://doi.org/10.11583/DTU.30094420.v1

[25] Gaertner, E., Rinker, J., Sethuraman, L., Zahle, F., Anderson, B., Barter, G.E., Abbas, N.J., Meng, F., Bortolotti, P., Skrzypinski, W. and Scott, G.N., 2020. IEA wind TCP task 37: definition of the IEA 15-megawatt offshore reference wind turbine (No. NREL/TP-5000-75698). National Renewable Energy Lab. (NREL), Golden, CO (United States).